

# Laser-induced emf in the quasi-one-dimensional conductor TaS<sub>3</sub>

M. E. Itkis, F. Ya. Nad', and V. Ya. Pokrovskii

*Institute of Radio Engineering and Electronics, Academy of Sciences of the USSR*

(Submitted 18 July 1985)

*Zh. Eksp. Teor. Fiz.* **90**, 307–317 (January 1986)

An anomalous emf has been observed in the quasi-one-dimensional conductor TaS<sub>3</sub> during illumination with a narrow laser beam. This emf results from temperature gradients induced by the beam. The magnitude and sign of the emf depend on the coordinate of the point at which the sample is illuminated. This dependence exhibits hysteresis as the beam direction is reversed. After the application of a voltage pulse  $V_a$  above a threshold, the magnitude of the emf changes. This change has different values, depending on the polarity of  $V_a$ ; i.e., here again there is a hysteresis. The magnitude of the emf relaxes with time in accordance with  $\mathcal{E} \propto \lg t$ . A model proposed here gives a qualitative description of the effect of the temperature and electric field on the incommensurate charge density wave in a quasi-one-dimensional conductor. This model is used to explain the observed behavior and to extract the spatial distribution of the residual deformation of the charge density wave from the experimental data.

## I. INTRODUCTION

The basic properties of quasi-one-dimensional (Q1D) conductors are determined by the presence of a gap in the energy spectrum (a Peierls gap) and by electrons which have condensed into a charge density wave.<sup>1</sup> Charge density wave excitations of the ground state of a Q1D conductor i.e., quasiparticles (electrons and holes), and also solitons govern the optical properties and the conductivity in a weak electric field  $E$ , below a threshold field  $E_T$  (Ref. 2). The ground state of a real Q1D conductor (the charge density wave, its amplitude  $\Delta$ , and its phase  $\varphi$ ) is strongly affected by such effects as pinning at impurities, contacts, and the original lattice (commensurability<sup>3–6</sup> and by the existence of metastable states in which the charge density wave “remembers” earlier influences, including those which give rise to a nonuniform deformation of the charge density wave.<sup>10,11</sup> The greatest changes occur in the phase of the charge density wave and in turn cause changes in many macroscopic properties of the Q1D conductor. In orthorhombic TaS<sub>3</sub>, one of the typical Q1D conductors, these changes also lead to experimentally observable effects, such as hysteresis in the dependence of the electrical conductivity on the temperature<sup>12</sup> and the electric field,<sup>8,9</sup> a “memory” of the sign of the applied voltage,<sup>13</sup> and a residual deformation of the charge density wave.<sup>10,11</sup> Despite the large number of theoretical and experimental papers on the subject, the physical nature of many of these effects has not been finally resolved.

In the present paper we report a study of the effect of a narrow laser beam on TaS<sub>3</sub> at temperatures  $\sim 100$  K. The results show that an emf arises at the contacts on TaS<sub>3</sub> samples because of the nonuniform temperature distribution along the sample. The dependence of the magnitude of the emf on the direction in which the beam is moved along the sample and on the polarity of a voltage applied beforehand shows a hysteresis. We have studied the relaxation time of this emf. We propose a model which gives a qualitative explanation of the observed effects. We use this model to deter-

mine the spatial distribution of the residual deformation of a charge density wave from the experimental data.

## 2. EXPERIMENTAL APPARATUS

The orthorhombic TaS<sub>3</sub> samples have a Peierls transition temperature  $T_p = 217$ – $220$  K and threshold fields  $E_T \approx 0.3$ – $1.0$  V/cm. For the measurements we selected thin crystals with a cross-sectional area  $\approx 1 \mu\text{m}^2$  and a length of 1–3 mm. The samples were mounted on a sapphire substrate with cold indium solder.<sup>14</sup> The sample rested on indium contacts and is raised slightly above the substrate (Fig. 1), so that as the central part of the sample was heated the heat was removed primarily through the sample toward the contacts and then into the substrate. The heat removal from the surface of the sample is estimated to be small in the vacuum  $\approx 10^{-3}$  torr. The measurements in the temperature range

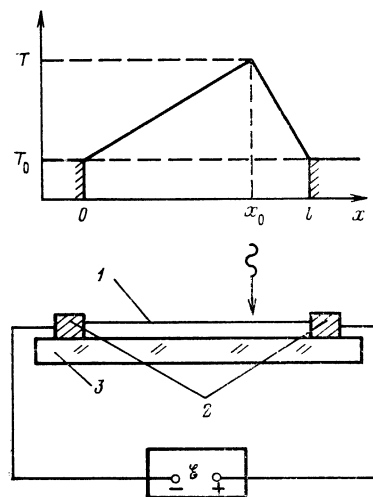


FIG. 1. Arrangement for measuring the emf. 1—Sample; 2—indium contacts; 3—sapphire substrate. Shown at the top is the temperature distribution along a sample of length  $l$  at it is illuminated at the point  $x_0$ .

90–300 K were carried out in an optical cryostat. The temperature of the sapphire substrate was measured with a calibrated silicon diode. The relative error of the measurements and regulation of the temperature during the measurements was  $\pm 0.1$  K.

A narrow beam ( $\approx 15 \pm_{5}^{10} \mu\text{m}$ ) from a helium-neon laser, with a wavelength of  $0.63 \mu\text{m}$ , was directed onto the sample. The beam was moved over the sample by a micrometer drive at the focusing lens (the positioning precision was  $\sim 10 \mu\text{m}$ ). The sample was shielded from background illumination by a cold copper screen with a narrow slit through which the laser beam enters. In measurements of the dependence of the magnitude of the emf on the light wavelength ( $\lambda = 1\text{--}14 \mu\text{m}$ ) we used a prism monochromator. The emf which arose during the laser irradiation was measured by a sensitive nanovoltmeter with a high-resistance input ( $R_{\text{in}} \approx 30 \text{ M}\Omega$ ; Fig. 1). The error in the emf measurements was determined by the zero drift and the drift of the input current of the nanovoltmeter; it was less than  $\pm 1 \mu\text{V}$ .

### 3. EXPERIMENTAL RESULTS

We found that an emf  $\mathcal{E}$  arises in all of the  $\text{TaS}_3$  samples studied ( $T < T_p$ ) when they are illuminated with the laser beam (or from a beam from a monochromator), at a zero bias voltage. The magnitude of this emf increases linearly with increasing power of the laser beam incident on the sample, up to  $\sim 10^{-7}$  W. At higher power levels, there is a tendency for the increase in  $\mathcal{E}$  to reach saturation. The spectrum of the emf in the interval  $1\text{--}14 \mu\text{m}$  is similar to that of the bolometric response of a  $\text{TaS}_3$  sample<sup>15</sup> The magnitude of the emf and its polarity with respect to the input terminals of the measurement instrument (Fig. 1) depend on the position of the point at which the sample is illuminated. The sign of the emf at the electrode nearest the point of illumination is always positive (more on this below). The magnitude of the emf also depends strongly on the temperature. Above  $T_p$ , the emf is low, less than  $\sim 0.1 \mu\text{V}$  at an incident power  $\approx 10^{-7}$  W. As the temperature is lowered, we observe near  $T_p$  a slight local maximum, which is followed by an increase in the emf to a maximum  $\sim 100 \mu\text{V}$  at 115 K and then a decrease. When the temperature is instead raised, the magnitude of the emf is lower at a given temperature; i.e., there is a significant thermal hysteresis. A hysteresis was recently detected<sup>16</sup> in the temperature dependence of the ordinary thermoelectromotive force of  $\text{TaS}_3$ ,

The emf which we observe might be due to either the thermal effect of the laser irradiation or photoelectric (nonthermal) effects at contacts or inhomogeneities of the sample, e.g., a depletion-layer rectification. To help choose between these two possibilities, we carried out some further experiments. First, we measured the emf of a laser-irradiated sample placed directly on a substrate of a good heat conductor, sapphire. In these experiments, thin  $\text{TaS}_3$  samples ( $\approx 1 \mu\text{m}$  in diameter) were in close contact with the surface of the sapphire substrate, for good heat removal from the sample. We found in these experiments that the magnitude of the emf was reduced by a factor of about 100 from that found when

the sample was in its ordinary position above the substrate (Fig. 1). In this case, photoelectric (nonthermal) effects should not have changed substantially. In a second experiment we measured the relaxation time of the observed emf during pulsed irradiation of the sample. We found a relaxation time  $\sim 10^{-2}$  s, in good agreement with the thermal relaxation times customarily observed for photoelectric effects. Consequently, the sharp decrease in the emf in samples clamped to the substrate, the typical spectrum of the emf, which corresponds to a bolometric response,<sup>15</sup> and the significant inertia of the emf show that the observed emf was due to a heating of the sample.

Special experiments were carried out to determine the temperature distribution over the sample during nonuniform illumination of the sample with a laser beam. The end of a second  $\text{TaS}_3$  sample, shielded from the radiation and serving as a microthermometer, was pressed against one of the contacts on the test sample. The change in the temperature of the contact common to the two samples was determined from the magnitude of the ordinary thermoelectromotive force ( $\approx 800 \mu\text{V/K}$ ; Refs. 16 and 17) in the unilluminated sample. It was found that during illumination of the indium-coated contact alone that the temperature of this contact with respect to the unilluminated contact increased by about  $10^{-2}$  K. This heating corresponded to the appearance of an ordinary thermoelectromotive force  $\sim 10 \mu\text{V}$  at the microthermometer. As the beam was moved along the sample, the temperature difference between the contacts was also less than  $10^{-2}$  K. It fell off linearly with distance from the beam to the common contact. This linear behavior of the contact temperature and also the small amount of heat removed from the surface of the sample in comparison with the heat removal at the contacts are evidence that the temperature distribution along the sample is as shown in Fig. 1, with a maximum at the illumination point  $x_0$  and with linear decays toward the contacts. An estimate of the heating of the illuminated part of the sample based on the change in the resistance of the sample at a constant temperature showed that the temperature of this region rose by about 10 K.

The emf which we observed however, could not be a direct consequence of the ordinary thermoelectromotive force which arises from a temperature difference. When the end temperature of a homogeneous sample are equal (in our case, we have  $\Delta T < 10^{-2}$  K), regardless of the temperature distribution between the ends, the ordinary thermoelectromotive force in the sample is known to be zero. Furthermore, the ordinary thermoelectromotive force which arises during the heating of a blackened contact by a beam corresponds to  $p$ -type conductivity (with the minus side at the heated end). When a part of the sample near the same contact is illuminated, the sign of the emf which we measure reverses. The temperature distribution along the sample described above could in principle give rise to an emf by virtue of a difference in temperature gradients (the Benedics effect<sup>18</sup>) or the presence of irregularities in the sample.

We were accordingly interested in studying the change in the emf between the ends of the sample as the position  $x_0$  of the beam along the sample was varied. In most of the samples the behavior was found to be as shown in Fig. 2. As the

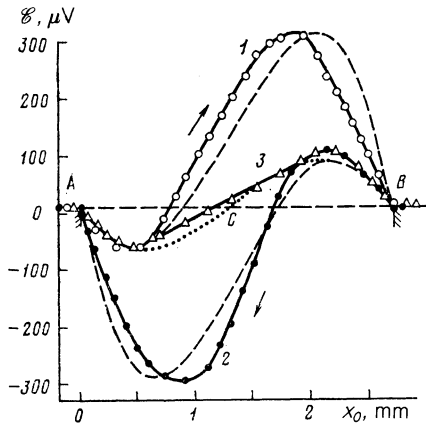


FIG. 2. Magnitude of the emf versus the coordinate of the point at which the sample is illuminated,  $x_0$ , at  $T = 125$  K. Curve 1 (O)—Recorded as the laser beam is moved from contact  $A$  to contact  $B$ ; curve 2 (●)—as the beam is moved in the opposite direction, from  $B$  to  $A$ ; dashed curves—corresponding theoretical results; 3 ( $\Delta$ ) equilibrium curve and corresponding calculated curve (dotted curve), found from expression (1).

beam is moved from contact  $A$  to contact  $B$  (curve 1), there is a smooth in  $\mathcal{E}$ , in the form of an asymmetric wave with a minimum and a maximum. When the beam is moved in the opposite direction, from  $B$  to  $A$ , the values of the emf lie on curve 2, whose shape correspond to the mirror image of curve 1 around point  $B$ . The difference between the curves (the magnitude of the hysteresis) increases with increasing light intensity. The direction around the loop is the same for all the samples. These curves were found during the motion of a cw beam; if, after the beam is moves to some point on the sample, it is turned off longer than a few seconds and then turned on again, the emf values  $\mathcal{E}_0$  lie on curve 3 (Fig. 2) and are independent of the direction in which the beam is moved, within the experimental error. The greater symmetry of curve 3 with respect to a zero level of the emf (with the laser turned off) and the absence of hysteresis here allow us to adopt this curve as a sort of "equilibrium" curve with respect to the nonequilibrium curves 1 and 2. The same sort of curve, without hysteresis, is found if at each point, before a measurement of the emf, an alternating voltage ( $f \approx 1$  Hz) with a gradually decreasing amplitude and an initial value  $V \approx 4V_T$  ( $V_T$  is the threshold voltage) is applied to the sample instead of turning off the beam.

In the samples which we studied, the position of the point at which the equilibrium curve crosses the zero level (point  $C$  in Fig. 2) is displaced somewhat from the middle of the sample. In most of the samples, the displacement amounts to between 2% and 8% of the length of the sample, but in a few samples it was far larger. We will call these "homogeneous" and "inhomogeneous" samples, respectively. In the inhomogeneous samples, there are structural features on the  $\mathcal{E}_0(x_0)$  curves associated with the positions of inhomogeneities. The asymmetry of the  $\mathcal{E}_0(x_0)$  curve is also significantly more pronounced, but it is qualitatively the same for all the curves. The inhomogeneous samples show a greater sensitivity to the background radiation in the room and to a uniform illumination of the entire sample. For example, in a homogeneous sample the emf from the back-

ground (the zero level) is usually less than  $\sim 20 \mu\text{V}$ , while in an inhomogeneous sample it can reach  $\sim 500 \mu\text{V}$ . Its magnitude is proportional to the degree of asymmetry of the  $x_0$  dependence of the emf, and its sign corresponds to the sign of the larger  $\mathcal{E}_0(x_0)$  half-wave (Fig. 2).

It might also be suggested that some of the inhomogeneities in the sample stem from the mechanical deformation of the  $\text{TaS}_3$  crystal near its contacts. To test this possibility we carried out an experiment in such a way that the region with the temperature gradient was shifted away from the contacts. For this purpose the sample rested on a substrate over a distance  $\sim 1$  mm near its contacts, while at its center, over a distance  $\sim 2.5$  mm, it hung freely over a notch in the substrate. As a result, when the regions near the contacts, in good thermal contact with the substrate, were illuminated, there was no emf, but when the central part was illuminated a curve similar to the equilibrium curve in Fig. 2 was reproduced. These results indicate that there is no relationship between the observed emf and a possible mechanical deformation of the sample near its contacts.

The emf which we studied was of course measured when no external voltage  $V$  of any sort was applied to the sample. It turns out, however, that the magnitude of the emf depends strongly on the magnitude and direction of a potential applied beforehand,  $V_a$  (Fig. 3a). The points in this figure were obtained in the following way. We first applied a voltage considerably above the threshold voltage  $V_T$  (e.g.,  $-800$  mV) to the illuminated sample, then removed this voltage abruptly, and then measured the emf a few seconds later. We then repeated the emf measurements after each application of the voltage, with an amplitude which was gradually reduced to zero, then increased to  $+800$  mV (the lower curve in Fig. 3a), and then reduced again to  $-800$  mV (the upper curve). Figure 3b shows the differential conductivity  $\sigma_d$  versus the voltage across the sample. On the  $\sigma_d(V)$  curve we see some small jumps between  $0.5V_T$  and  $V_T$ .

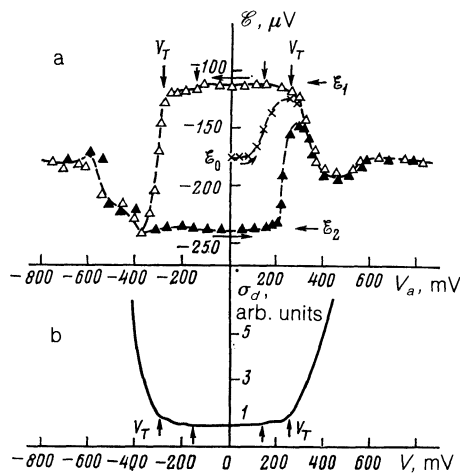


FIG. 3. a: Magnitude of the emf versus the voltage applied beforehand,  $V_a$ .  $\blacktriangle$ —Sequence of changes in  $V_a$  from  $-800$  to  $+800$  mV;  $\Delta$ —from  $+800$  to  $-800$  mV;  $\times$ —motion from the equilibrium value  $\mathcal{E}_0$ . b: The differential conductivity  $\sigma_d$  versus the voltage. Arrows—structural features on the curves of  $\mathcal{E}(V_a)$  and  $\sigma_d(V)$ ;  $V_T$ —threshold voltage ( $T = 125$  K).

It can be seen from Fig. 3a that there is a clearly expressed hysteresis in the plot of the emf versus the voltage applied beforehand. The values of the emf found after the application of a voltage  $V_a > (1.5-2)V_T$  are essentially independent of the magnitude of  $V_a$  and of the sign of the voltage; they are approximately equal to the values of  $\mathcal{E}_0$  corresponding to the middle of the hysteresis loop. At voltages  $V_a \ll V_T$  there are two stable and quite different states in the sample,  $\mathcal{E}_1$  and  $\mathcal{E}_2$  (Fig. 3a). The transition to these states depends on the direction in which the voltage is changed (the history): The state  $\mathcal{E}_1$  is reached when we go from plus to minus, while  $\mathcal{E}_2$  is reached when we go from minus to plus. At voltage  $V_a \approx V_T$  there is a transition region between  $\mathcal{E}_1$  and  $\mathcal{E}_2$ . It can be seen from Fig. 3 that the curves of  $\mathcal{E}(V_a)$  at  $V_a < V_T$  have structural features which correlate with the  $\sigma_a(V)$  curve. In all the samples, for various positions of the laser beam on the sample, the direction along which the hysteresis loop is traced out is the same. The polarity of the increment in the emf  $\mathcal{E}_0$  which arises is the same as that of the voltage applied beforehand to the sample. Higgs<sup>16</sup> has mentioned a slight change in the magnitude of the ordinary thermoelectromotive force after a current above a threshold is passed through a sample.

The temperature dependence of the width of the field hysteresis loop and that of the hysteresis loop from the direction of the motion of the beam have a maximum near a temperature of 115 K. As the temperature is raised or lowered from 115 K, the magnitude of the hysteresis decreases, more rapidly in the case of the field hysteresis. The  $\mathcal{E}(V_a)$  curves were measured during continuous illumination of a point on the sample by the laser beam. If, after each application of the field the beam was blocked (and the sample cooled down) and then unblocked (the sample warmed up), the resulting  $\mathcal{E}(V_a)$  curve again shows the same type of hysteresis, but the hysteresis loop is smaller. The measurements of the nonequilibrium emf after the displacement of the beam or after the application of the voltage pulse were usually carried out in a time  $\sim 1$  min. Special measurements of the time evolution of the magnitude of the nonequilibrium emf over several hours showed that the emf slowly relaxes approximately by  $\mathcal{E} \propto \lg t$ . These results agree qualitatively with the results of measurements of the relaxation of metastable states formed in TaS<sub>3</sub> as the result of a thermal agent<sup>19</sup> or a field.<sup>20</sup>

#### 4. DISCUSSION OF RESULTS

It follows from these experimental results that the laser illumination of homogeneous TaS<sub>3</sub> single crystals gives rise to an emf which depends on the point on the sample which is illuminated and on the magnitude of an electric field applied beforehand. This emf is caused by a nonuniform heating of the sample by the electromagnetic radiation. It was shown above that the basic features of these effects cannot be attributed to a temperature difference between the ends of the sample, since this difference is  $\Delta T < 10^{-2}$  K; nor can it be attributed to the initial inhomogeneity of the structure and of the properties of the sample. To explain these results, let us examine the changes which occur with a charge density wave in a Q1D crystal when temperature gradients and an

electric field are applied to it.

We know that in many Q1D materials, e.g., NbSe<sub>3</sub>, K<sub>0.3</sub>MoO<sub>3</sub>, and orthorhombic TaS<sub>3</sub>, the charge density wave in the temperature region studied,  $T > 100$  K, is in a state near commensurability.<sup>21,22</sup> In TaS<sub>3</sub>, the component of the wave vector  $\mathbf{q}$  of the charge density wave along the axis of the highest conductivity,  $\mathbf{c}$  decreases with decreasing temperature in this region, until a transition to a fourfold commensurability occurs.<sup>21</sup> It follows that as the temperature along a TaS<sub>3</sub> sample is varied a corresponding spatial variation in  $\mathbf{q}$  will also arise in it. Recent experiments have also revealed a change in the vector  $\mathbf{q}$  ( $\delta q/q \approx 1\%$ ), depending on the magnitude and direction of an electric field.<sup>22</sup> No change was observed in the amplitude  $\delta\Delta$  of the charge density wave within experimental error, was observed. It can also be concluded from the existing theory (Ref. 5, for example) that we have  $\delta\Delta \propto (\delta q)^2$  and that this quantity should be small for small changes in  $\mathbf{q}$ . On the other hand, using the expression  $\Delta = \Delta_0 \cos [qx + \varphi(x)]$ , for the charge density wave, we can easily show that the phase gradient satisfies  $d\varphi/dx \propto \delta q(x)$ . We know that a phase gradient of a charge density wave means the appearance of additional charges with the density  $\delta\rho(x) \propto d\varphi/dx$ , distributed over the sample. In our case of an incommensurate charge density wave, the continuous change in phase is preferable to an abrupt change in phase of  $2\pi$ , which corresponds to the appearance of phase solitons in a charge density wave and to regions of incommensurability ("discommensurations"), which separate regions of a commensurate charge density wave.<sup>23,24</sup> Regardless of the details of the complex changes in  $\varphi(x)$ , the point of importance to us is the fact that an additional charge, e.g., solitons of charge  $2e$ , appears near the phase jump.<sup>23</sup> In real crystals, these solitons may attach to impurities and defects. A natural consequence of such changes would be a coordinate-dependent shift of the chemical potential  $\mu$  in a crystal.

Our experimental results can be explained satisfactorily in this model. We showed in Section 3 that under our experimental conditions the temperature distribution along the sample has the form shown in Fig. 1 and that the emf which we observed might be due to the presence, in a homogeneous sample, of two temperature gradients, of opposite sign and with magnitudes depending on the point at which the sample is illuminated. A similar effect (the Benedics effect<sup>18</sup>) can be observed in a semiconductor if the carrier diffusion length  $L_D$  is comparable to the length scale for the change in the carrier density in a region with a temperature gradient,<sup>18</sup>  $L_0 \propto \nabla T/T$ . The changes ( $\Delta n$ ) in the carrier density and thus the values of  $\delta\mu(x)$  in a sense lag behind the temperature changes. The differential thermoelectromotive force  $S_0$  becomes a function not only of the temperature but also of the temperature gradients, giving rise to a nonvanishing emf in a sample with different contact temperature but with gradients of equal magnitudes. It follows from Ref. 18 that in an intrinsic semiconductor we would have

$$\mathcal{E}_0 \sim [(L_D/L_{01})^2 - (L_D/L_{02})^2](T - T_0), \quad (1)$$

where  $L_{01,2}$  refer to the regions with the gradients of the opposite signs. In TaS<sub>3</sub>, however, because of the low mobili-

ties<sup>25</sup> and short free-carrier lifetimes (shown by the absence of photoconductivity<sup>15</sup>), the corresponding diffusion length is short ( $L_D/L_0 \ll 1$ ). The emf calculated from Ref. 18 is found to be many orders of magnitude lower than that observed experimentally. This result apparently indicates that the simple semiconductor picture<sup>18</sup> is not applicable to Q1D TaS<sub>3</sub>, and the specific properties of a charge density wave must be taken into account.

In Q1D crystals, as we showed above, the change in  $q$  in the region with the temperature gradient gives rise to a phase gradient of the charge density wave and to a change in the charge density, with the result that there is a shift of the chemical potential,<sup>26,27</sup>  $\delta\mu \propto d\varphi/dx$ . As in the case of a semiconductor,  $S_0$  becomes a function of the temperature gradients, so that something akin to a Benedics effect may occur. The role of the diffusion length  $L_D$  in (1) is played by the distance over which the charge density wave loses its phase coherence. This so-called Fukuyama-Lee-Rice length  $L_{FLR}$  (Ref. 28) is set by the average interaction with impurities. For TaS<sub>3</sub>, it is 10–100  $\mu\text{m}$ . Under these assumptions, an estimate of the emf  $\mathcal{E}_0$  on the basis of the expression for the Benedics emf<sup>18</sup> yields values in order-of-magnitude agreement with experiment. The dependence  $\mathcal{E}_0(x_0)$  constructed on the basis of an expression of type (1) (Ref. 18) agrees qualitatively with the experimental equilibrium curve 3 in Fig. 2.

The hysteresis in the plot of  $\mathcal{E}_0$  versus the position of the illumination point on the sample (curves 1 and 2 Fig. 2) results from the existence of metastable states in TaS<sub>3</sub> as the temperature is varied.<sup>8,9,12</sup> As the beam is moved along the sample (curve 1 in Fig. 2), in the regions traversed by the beam the vector  $q$  remains in metastable states which “remember” the preceding temperature conditions (a thermal hysteresis). Consequently, just after the beam passes through such a region of the sample there is a “superheated” region with nonequilibrium values  $q_0 + \delta q(x)$  and  $\mu_0 + \delta\mu(x)$  and with an increment  $\delta S(x)$  which increases the emf:

$$\mathcal{E} \propto \int_0^l \delta S(x) \nabla T dx.$$

A calculation incorporating the temperature distribution and the nature of the thermal hysteresis<sup>8</sup> leads to a functional dependence  $\mathcal{E}(x)$  which agrees qualitatively with experiment (Fig. 2). When the beam is moved in the opposite direction (curve 2 in Fig. 2), the sign of the temperature gradient in the “superheated” region changes, giving us an effect of the opposite sign.

It can be seen from Fig. 3 that the application of a voltage  $V_a$  before the measurement of the emf has an important effect on the magnitude of the emf. To explain this effect, we can again use the model described above. The electric field causes a deformation of the charge density wave, changing its wave vector  $q$  (Refs. 11 and 22). After the field is removed, the pinning at impurities in the charge density wave may result in the preservation of a residual deformation which depends on  $x$ , with corresponding phase gradients, altered values  $q_0 + \delta q(V_a)$  and  $\mu_0 + \delta\mu(V_a)$ , and a differential thermoelectromotive force  $S_0 + \delta S(V_a)$ . A change in

the temperature along a sample with different values of  $\delta S(V_a, x)$  can give rise to a nonzero emf  $\mathcal{E}_V$  of the ordinary kind (i.e., one which depends on  $\Delta T$ , not on  $\nabla T$ ) at the contacts on the sample. This emf is added to the existing emf  $\mathcal{E}_0$  due to the temperature gradients.

The hysteresis in  $\mathcal{E}(V_a)$  (Fig. 3) is explained in the following way. The application of a voltage  $V_a \gg V_T$  causes a motion of the charge density wave as a whole. In the course of this motion, the charge density wave is actually very insensitive to the impurity potential; its correlation length is large; and a noticeable deformation is limited to small regions near the contacts, where a phase slippage occurs.<sup>5,29</sup> After the voltage is turned off abruptly, the charge density wave becomes attached to impurities as a slightly deformed wave, nearly the same as the wave before the voltage was turned off. In this situation hysteresis is essentially absent at  $V_a \gtrsim (3-4)V_T$ , the values of  $\mathcal{E}(V_a)$  agree for large positive and negative voltages  $V_a$ , and these voltages are close to the center of the loop, i.e., to the value of  $\mathcal{E}_0$  (Fig. 3). As  $V_a$  is reduced, the hysteresis becomes greater in magnitude, reaching its highest values at  $V_a \gtrsim V_T$ . This results means that in this region of  $V_a$  the residual deformation of the charge density wave and the value of  $\delta q$  are maximized. The reversal of the voltage polarity changes the sign of the deformation of the charge density wave and of  $\delta q$  without significantly changing their amplitudes, with the result that we have a symmetric hysteresis loop (Fig. 3). These results agree qualitatively with the data of Ref. 11, where a change in the electrical conductivity of regions of a sample was observed after the application of the voltage  $V > V_T$ .

Voltages  $V_a \ll V_T$  cannot displace the charge density wave or substantially deform it. In the region  $V_T/2 \lesssim V \lesssim V_T$ , however, there may be some redistribution of metastable states of the charge density wave, according to our data (Fig. 3). The result is a change in  $\mathcal{E}(V_a)$  which is correlated with corresponding changes on the  $\sigma_d(V)$  curve. The possibility of a charge density  $V_T/2 \leq V \leq V_T$  was also mentioned in Refs. 8 and 30.

It is natural to suggest that the half-width of the hysteresis loop,  $\mathcal{E}_V(0) = (\mathcal{E}_1 - \mathcal{E}_2)/2$  (Fig. 3) is proportional to the magnitude of the residual deformation of the charge density wave and to the corresponding change in the chemical potential  $\delta\mu(V_a)$  after the application of a voltage  $V_a \gtrsim V_T$ . By moving the beam along the sample and measuring the half-width of the  $\mathcal{E}_V(0, x_0)$  loop at each point, we can directly find the spatial distribution of  $\delta S(x) \sim \delta\mu(x)$ —i.e., ultimately, the distribution of the residual deformation of the charge density wave along the sample. For the temperature distribution in Fig. 1, with

$$T - T_0 = \begin{cases} (1-x_0)x & \text{for } x < x_0 \\ x_0(1-x) & \text{for } x > x_0 \end{cases}, \quad (2)$$

we find

$$\mathcal{E}_V(x_0) = \int_0^{x_0} \delta S(x) dx - x_0 \int_0^1 \delta S(x) dx, \quad (3)$$

$$\frac{d\mathcal{E}_V(x_0)}{dx_0} = \delta S(x_0) - \int_0^1 \delta S(x) dx, \quad (4)$$

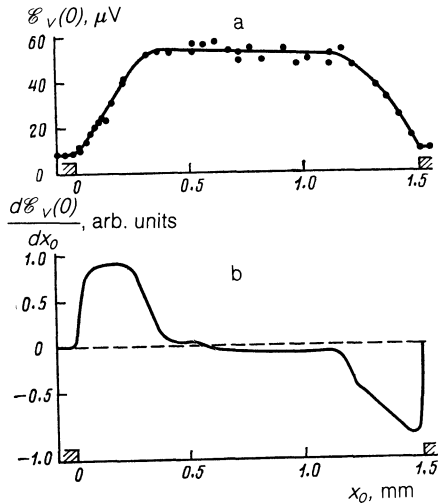


FIG. 4. a—Half-width of the field-induced hysteresis loop,  $\mathcal{E}_V(0) = (\mathcal{E}_1 - \mathcal{E}_2)/2$  versus the coordinate of the point at which the sample is illuminated,  $x_0$ ; b—dependence of  $d\mathcal{E}_V(0)/dx_0$  on the coordinate of the point at which the sample is illuminated. This dependence determines the distribution of the residual deformation of the charge density wave.

where  $x_0$  and  $x$  are coordinates, divided by the length of the sample,  $l$  (Fig. 1),  $\delta S(x)$  is the change in the differential thermoelectromotive force caused by  $V_a$ , and the second term in (4) is a constant, independent of  $x_0$ .

Figure 4 shows the half-width of the  $\mathcal{E}_V(0)$  hysteresis loop as a function of the coordinate  $s_0$ , along with the derivative of this function. We see that the quantity  $\delta S(x)$  and thus  $d\varphi/dx$  and the residual deformation of the charge density wave have different signs at the contacts: the charge density wave is compressed near one contact and extended near the other. The deformation is a maximum near the contacts and usually extends over macroscopic regions,  $\sim 300\text{--}400\ \mu\text{m}$ . On occasion, it spans the entire sample ( $l \sim 1\ \text{mm}$ ), changing sign at the center of the sample. In some of the samples we observe a sharp change  $\delta S(x)$  in the immediate vicinity of the contacts, at distances less than  $50\ \mu\text{m}$ . A detailed study of this effect will require increasing the resolution of the method, primarily by decreasing the diameter of the laser beam. It is important to note that the distribution of the deformation of the charge density wave found in this manner does not depend on the intensity of the light (for a temperature drop  $< 10\ \text{K}$  in the sample), and the width of the hysteresis loop increases linearly with the intensity.

Corresponding to the distribution found for  $\delta S(x)$  are the curves of  $\varphi(x)$ ,  $d\varphi(x)/dx$  and  $\delta\mu(x)$  sketched in Fig. 5. The regions of extension and compression of the charge density wave naturally correspond to regions with phase gradients of opposite signs, additional charges of opposite signs, and corresponding shifts of the chemical potential. "Doping" of the sample occurs, accompanied by the appearance of  $n$ -type and  $p$ -type regions, controlled by the voltage  $V_a$ . This doping might be represented as a consequence of the formation of localized states (defects in a superlattice) within the Peierls gap, analogous to impurities in semiconductors which are associated with phase jumps (solitons) or regions

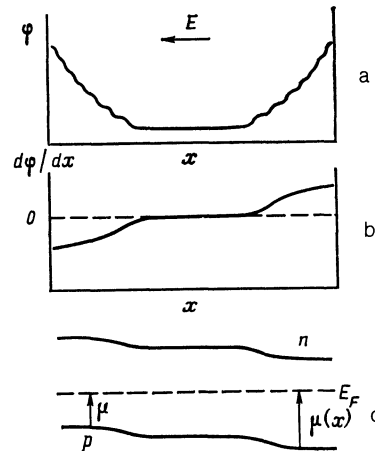


FIG. 5. Schematic spatial distributions of (a) the charge density wave, (b) the phase gradient (the smoothed curve), and (c) the shift of the chemical potential.

of an incommensurability of the charge density wave. The residual changes in electrical conductivity observed in Ref. 11 could be explained in the same way.

According to our measurements (Section 3) and also according to the data of Refs. 19 and 20. The relaxation of the residual deformations of the charge density wave occurs logarithmically, and the time required to halve the emf is more than  $10^3\ \text{h}$ . A relaxation of this nature correlates with the frequency dependence of the electrical conductivity in  $\text{TaS}_3$ ,  $\sigma(\omega) \propto \omega^{0.8}$  (Ref. 31), and occurs because this material has a wide spectrum of potential-barrier heights and of corresponding times for transitions between different metastable states (as in Fermi glasses).

We wish to thank S. N. Artemenko, S. A. Brazovskii, A. F. Volkov, and T. M. Lifshitz for a discussion of these results. We also thank Ya. S. Savitskaya for furnishing the samples.

- <sup>1</sup>J. J. Andre, A. Bieber, and F. Gauter, *Ann. Phys. (Paris)* **1**, 145 (1976).
- <sup>2</sup>Gy. Hutiray and J. Sölyom (editors), *Proceedings of the International Conference on Charge Density Wave in Solids*, Budapest, Hungary, 1984. Lecture Notes in Physics, Springer-Verlag, Berlin (1985), vol. 217.
- <sup>3</sup>P. A. Lee and T. M. Rice, *Phys. Rev.* **B19**, 3970 (1979).
- <sup>4</sup>N. P. Ong and G. Verma, *Phys. Rev.* **B27**, 4495 (1983).
- <sup>5</sup>L. P. Gor'kov, *Pis'ma Zh. Eksp. Teor. Fiz.* **38**, 76 (1983) [*JETP Lett.* **38**, 67 (1983)]; *Zh. Eksp. Teor. Fiz.* **86**, 1818 (1984) [*Sov. Phys. JETP* **59**, 1057 (1984)].
- <sup>6</sup>S. N. Artemenko and A. F. Volkov, *Zh. Eksp. Teor. Fiz.* **81**, 1872 (1981) [*Sov. Phys. JETP* **54**, 992 (1981)].
- <sup>7</sup>J. C. Gill, *Solid State Commun.* **39**, 1203 (1981).
- <sup>8</sup>Gy. Hutiray, G. Mihály and L. Mihály, *Solid State Commun.* **47**, 737 (1983); **48**, 203 (1983).
- <sup>9</sup>M. E. Itkis and F. Ya. Nad', *Tezisy dokladov Vsesoyuznogo simpoziuma "Neodnorodnye elektronnye sostoyaniya"* (Proceedings of the All-Union Symposium on Inhomogeneous Electron States), Novosibirsk, 1984, p. 136.
- <sup>10</sup>A. Jánossy, G. Mihály, and G. Kriza, *Solid State Commun.* **51**, 63 (1984).
- <sup>11</sup>L. Mihály and A. Jánossy, *Phys. Rev.* **B30**, 3530 (1984).
- <sup>12</sup>A. W. Higgs and J. C. Gill, *Solid State Commun.* **47**, 737 (1983).
- <sup>13</sup>G. Mihály and L. Mihály, *Solid State Commun.* **48**, 449 (1983).
- <sup>14</sup>S. K. Zhilinskii, M. E. Itkis, N. Yu. Kal'nova, F. Ya. Nad', and V. B. Preobrazhenskii, *Zh. Eksp. Teor. Fiz.* **85**, 362 (1983) [*Sov. Phys. JETP* **58**, 211 (1983)].

- <sup>15</sup>M. E. Itkis and F. Ya. Nad', Pis'ma Zh. Eksp. Teor. Fiz. **39**, 373 (1984) [JETP Lett. **39**, 448 (1984)].
- <sup>16</sup>A. W. Higgs, in: Proceedings of the International Conference on Charge Density Wave in Solids, Budapest, Hungary, 1984. Lecture Notes in Physics, Springer-Verlag, Berlin (1985), vol. 217, p. 442.
- <sup>17</sup>B. Fisher, Solid State Commun. **46**, 227 (1983).
- <sup>18</sup>J. Tauc, Photoelectric and Thermoelectric Phenomena in Semiconductors (Russ. transl. IL, Moscow, 1962).
- <sup>19</sup>G. Mihály and L. Mihály, Phys. Rev. Lett. **52**, 149 (1984).
- <sup>20</sup>N. P. Ong, D. D. Duggan, C. B. Kalem, D. W. Jing, and P. A. Lee, in: Proceedings of the International Conference on Charge Density Wave in Solids, Budapest, Hungary, 1984. Lecture Notes in Physics, Springer-Verlag, Berlin (1985), vol. 217, p. 387.
- <sup>21</sup>Z. Z. Wang, H. Salva, P. Monceau, *et al.*, J. Phys. (Paris), **44**, L311 (1983).
- <sup>22</sup>T. Tamegai, K. Tsutsumi, S. Kadoshima, *et al.*, Solid State Commun. **51**, 585 (1984).
- <sup>23</sup>S. Brazovskii, N. Korova, and V. Yakovenko, J. Phys. (Paris) Colloq, **44**, 1525 (1983).
- <sup>24</sup>W. L. McMillan, Phys. Rev. **B14**, 1496 (1976).
- <sup>25</sup>Yu. I. Latyshev, Ya S. Savitskaya, and V. V. Frolov, Pis'ma Zh. Eksp. Eksp. Teor. Fiz **38**, 446 (1983) [JETP Lett. **38**, 541 (1983)].
- <sup>26</sup>I. E. Dzyaloshinskii and S. A. Brazovskii, Zh. Eksp. Teor. Fiz. **71**, 2338 (1976) [Sov. Phys. JETP **44**, 1233 (1976)].
- <sup>27</sup>S. N. Artemenko and A. F. Volkov, in: Proceedings of the International Conference on Charge Density Wave in Solids, Budapest, Hungary, 1984. Lecture Notes in Physics, Springer-Verlag, Berlin (1985), vol. 217, p. 188.
- <sup>28</sup>H. Fukuyama and P. A. Lee, Phys. Rev. **B27**, 535 (1978).
- <sup>29</sup>J. C. Gill, in: Proceedings of the International Conference on Charge Density Wave in Solids, Budapest, Hungary, 1984. Lecture Notes in Physics, Springer-Verlag, Berlin (1985), vol. 217, p. 377.
- <sup>30</sup>P. B. Littlewood, in: Proceedings of the International Conference on Charge Density Wave in Solids, Budapest, Hungary, 1984. Lecture Notes in Physics, Springer-Verlag, Berlin (1985), vol. 217, p. 369.
- <sup>31</sup>S. K. Zhilinskii, M. E. Itkis, and F. Ya. Nad', Phys. Status Solidi (a) **81**, 367 (1984).

Translated by Dave Parsons